Journal of Inflammation Research

Dovepress
Taylor & Francis Group

Open Access Full Text Article

ORIGINAL RESEARCH

Qijie Xiaopi Decoction Attenuates Gastric Mucosal Injury in PLGC Rats by Inducing Autophagy and Apoptosis Through PI3K/AKT/mTOR Pathway Inhibition

Yi Shan[1,2], Yang Ma[1,2], Hanfei Chen[1,2], Sichao Zhao[1,2], Mingzhu Shi[1,2], Min Bai[1,2], Junrui Hu[1,2]

[1]College of Traditional Chinese Medicine, Ningxia Medical University, Yinchuan, Ningxia Hui Autonomous Region, 750004, People's Republic of China; [2]Key Laboratory of Ningxia Ethnomedicine Modernization, Ministry of Education, Ningxia Medical University, Yinchuan, Ningxia Hui Autonomous Region, 750004, People's Republic of China

Correspondence: Junrui Hu; Min Bai, Email 89463882@qq.com; 1115487589@qq.com

Purpose: Precancerous lesions of gastric cancer (PLGC) represent a crucial juncture in the transformation from gastritis to gastric cancer. Qijie Xiaopi Decoction (QJXPD), a Chinese herbal medicine formulation that has been applied in clinical practice to manage PLGC, which is capable of effectively relieving the symptoms experienced by patients such conditions. However, its mechanism of action remains unclear. The aim of this study is to elucidate the mechanism of action of QJXPD in the treatment of PLGC.

Methods: Ultra-high-performance liquid chromatography coupled with hybrid quadrupole-orbitrap tandem mass spectrometry (UHPLC-Q-Exactive Orbitrap-MS) was employed to pinpoint the chemical components of QJXPD. On this basis, network pharmacology and molecular docking were employed to pinpoint the main ingredients, probable targets, and associated pathways of QJXPD in treating of PLGC. A PLGC rat model was replicated using a compound modeling method mainly based on N-methyl-N'-nitro -N-nitrosoguanidine (MNNG), to observe the therapeutic effects of QJXPD on PLGC.

Results: The undiluted QJXPD solution contained 1069 compounds. Network pharmacology analysis revealed that QJXPD's anti-PLGC effects involved 119 active ingredients and 332 potential targets, primarily enriched in the PI3K/AKT pathway. Protein-protein interaction (PPI) analysis suggested that TP53, AKT1, SRC, STAT3, and EGFR were the key targets. Through molecular docking, it was discovered that the core targets exhibited a strong binding affinity with the primary active ingredients. Animal experiments have verified that QJXPD can significantly improve the general condition in PLGC rats, increase body weight, repair the damaged gastric mucosa and diminish the inflammatory infiltration, induce apoptosis of gastric mucosal cells, upregulate the expression of LC3, Beclin-1, and Bax and downregulate the expression of p62 and Bcl-2. The PI3K/AKT/mTOR pathway was inhibited by QJXPD.

Conclusion: QJXPD effectively alleviated the pathological injury of gastric mucosa in PLGC rats by inhibiting the PI3K/AKT/mTOR signaling pathway and inducing cellular autophagy and apoptosis.

Keywords: Qijie Xiaopi decoction, precancerous lesions of gastric cancer, network pharmacology, PI3K/AKT /mTOR, autophagy, apoptosis

Introduction

Gastric cancer (GC) is regarded as one of the most common malignancies in the digestive system. According to data, in 2020, there were more than 1 million newly diagnosed cases of GC, and nearly 769,000 deaths related to it. Globally, it ranks as the fifth most prevalent malignant tumor and the fourth principal cause of cancer-related mortalities, this circumstance presents a severe peril to people's lives and well-being.[1] GC develops in accordance with the Correa cascade reaction model, the process begins with chronic superficial gastritis, progresses to chronic atrophic gastritis (CAG), is then followed by the emergence of intestinal metaplasia (IM) and dysplasia (Dys), and finally leads to the establishment of GC.[2] Precancerous Lesions of Gastric Cancer (PLGC) is a pathological concept that refers to the

Received: 12 May 2025
Accepted: 26 August 2025
Published: 31 August 2025

intestinal metaplasia and heterogeneous hyperplasia of the gastric mucosa on the basis of CAG, which is a transitional stage from "gastritis" to "gastric cancer",[3] blocking or delaying the progression of PLGC is an effective way to prevent and treat GC. Currently, Western medicine treats this disease with symptomatic treatment, mostly using drugs such as eradication of Helicobacter pylori, internal gastric mucosal protectants, and folic acid tablets, and combining surgical methods,[4] which lacks specific interventions. In the past few years, Traditional Chinese Medicine (TCM) therapy has gradually manifested its merits, which treats the PLGC state under the guidance of the holistic view and the theory of identification and treatment, and improves the symptoms of patients, even reversing the atrophy of glands, incomplete intestinal metaplasia, and dysplasia.[5]

Qijie Xiaopi Decoction (QJXPD) is a clinical-experience-based prescription evolved from Zhishi Xiaopi Pill, which is derived from "The Secret Treasury of the Orchid Chamber" written by Li Dongyuan and is a classic formula in TCM for treating digestive system diseases,[6,7] multiple studies have validated the efficacy of Zhishi Xiaopi Pills in treating PLGC.[8,9] QJXPD consist of 16 herbs: *Astragalus mongholicus* Bunge (Huangqi), *RESINA DRACONIS*. (Longxuejie), *Neolitsea cassia* (L). Kosterm. (Guizhi), *Smilax glabra* Roxb. (Fuling), *Paeonia lactiflora* Pall. (Baishao), *Perilla frutescens* (L). Britton (Zisugeng), *Citrus aurantium f. aurantium* (Zhishi), *Magnolia officinalis* Rehder & E.H. Wilson (Houpo), *Nardostachys jatamansi* (D. Don) DC. (Gansong), *Scleromitrion diffusum* (Willd). R.J. Wang (Baihuasheshecao), *Sepiella maindroni de* Rochebrune (Haipiaoxiao), *Fritillaria thunbergii* Miq. (Zhebeimu), *Kalanchoe pinnata* (Lam). Pers. (Sanqi), *Rheum officinale* Baill. (Dahuang), *Prunus mume* (Siebold) Siebold & Zucc. (Wumei), *Glycyrrhiza* glabra L. (Gancao). A data-mining research indicated that the frequently used TCM for treating PLGC encompass Huang Qi, Wu Mei and Bai Hua She She Cao, and others.[10] Currently, experiments have demonstrated that the key components of QJXPD can boost gastrointestinal motility, protect the mucosa, prevent carcinogenesis, and have potential therapeutic effects on PLGC. For instance, astragaloside IV regulates cell autophagy, effectively ameliorates gastric mucosal damage, and can even delay the progression of lesions.[11] Notoginsenoside effectively suppresses the inflammatory reaction in the gastric mucosa tissue and alleviates mucosal damage.[12] Triterpenoids help maintain the normal structure and function of the gastric mucosa and prevent the further deterioration of lesions.[13] Quercetin can effectively alleviate GC-related inflammation and optimize the tumor microenvironment.[14] The flavonoid luteolin can also treat gastric mucosal injury and inhibit gastric precancerous lesions by suppressing the STAT3/LCN2 axis.[15] Kaempferol exerts mucosal protection by modulating proinflammatory cytokines (TNF-α, IL-1β) and promoting NO synthesis.[16] The whole formula has the effects of invigorating the spleen, supplementing qi, removing blood stasis and detoxifying. Furthermore, it has shown favorable clinical effects and can ameliorate or even reverse the gastric mucosa's pathological alterations.[17] Nevertheless, the exact mechanism through which it mitigates PLGC remains elusive. The chemical composition represents a crucial aspect in elucidating the action mechanism and therapeutic efficacy of TCM. Liquid chromatography-mass spectrometry (LC-MS) integrates the ability of chromatography for rapid separation and mass spectrometry for mass analysis, and has been widely employed in analyzing intricate concoctions.[18] Network pharmacology represents a novel discipline that has emerged on the basis of systems biology theory. This particular discipline deploys bioinformatics and network analysis techniques to conduct in-depth analyses of biological systems, it can elucidate the molecular mechanisms of drugs through multiple targets in the network.

In recent years, many researches have shown that the pathogenesis of PLGC stems from the dysregulation of cell growth, proliferation, and apoptosis resulting from the combined effects of multiple factors and genes, and autophagy is involved in this biological process.[19] Investigations have shown that pre-cancerous cells are capable of utilizing autophagy as a strategic mechanism to mitigate inflammation and eliminate detrimental metabolites. This action serves as a safeguard, preventing the malignant transformation of cells.[20] As such, augmenting autophagy to modulate the equilibrium of the intracellular environment and enhance the cell's self-clearance capacity is of vital significance in impeding the onset and development of GC. Autophagy can either facilitate or impede apoptosis, and reciprocally, apoptosis can also either promote or suppress autophagy, the pathophysiology and progression of many diseases are closely linked to the intricate, reciprocal regulatory effects between autophagy and apoptosis.[21] The PI3K/AKT/mTOR pathway is one of the mechanisms involved in autophagy regulation,[22] it has been determined that this route is abnormally activated during the development of PLGC,[23,24] research has confirmed that TCM plays a protective role against gastric mucosal injury in PLGC, this may be associated with its regulation of cell autophagy and apoptosis via the

PI3K/AKT/mTOR pathway.[25] Therefore, targeted regulation of this pathway holds immense significance in forestalling the progression of GC.

In the present investigation, our primary objective was to clarify the underlying mechanism of QJXPD in treating PLGC. Firstly, the Ultra-high-performance liquid chromatography coupled with hybrid quadrupole-orbitrap tandem mass spectrometry (UHPLC-Q-Exactive Orbitrap-MS) was employed to pinpoint the active compounds of QJXPD. Subsequently, the key targets and related pathways through which QJXPD ameliorates PLGC were then predicted via network pharmacology and molecular docking. Finally, the potential mechanism was verified in in-vivo experiments using a PLGC rat model, providing experimental evidence in favor of TCM's clinical use. The schematic diagram of study is shown in Figure 1.

Materials and Methods

Animals

72 male Sprague-Dawley (SD) rats of specific pathogen-free (SPF) grade were procured from the Laboratory Animal Center of Ningxia Medical University. The animal production license number of this center is SYXK (Ning) 2020–0001. These experimental animals were housed in the SPF-grade laboratory (20–25 °C, 40–60% humidity, 12/12 h light and dark cycle) and fed a standard diet. After a 2-week adaptation period, experiments commenced. All animal procedures complied with the ethical principles of laboratory animals. The Animal Ethics Committee of Ningxia Medical University granted ethical approval for this experiment (IACUC-NYLAC-2023-198). The animal experiments were conducted in accordance with the Guide for the Care and Use of Laboratory Animals published by the National Research Council (NRC).

Drugs

Huangqi 15 g (2405002), Longxuejie 10 g (21100143), Guizhi 10 g (2406021), Fuling 10 g (YZ2404005), Baishao 12 g (230530–1), Zisugeng 12 g (2401009), Zhishi 12 g (2312016), Houpo 10 g (2403137), Gansong 12 g (2404001),

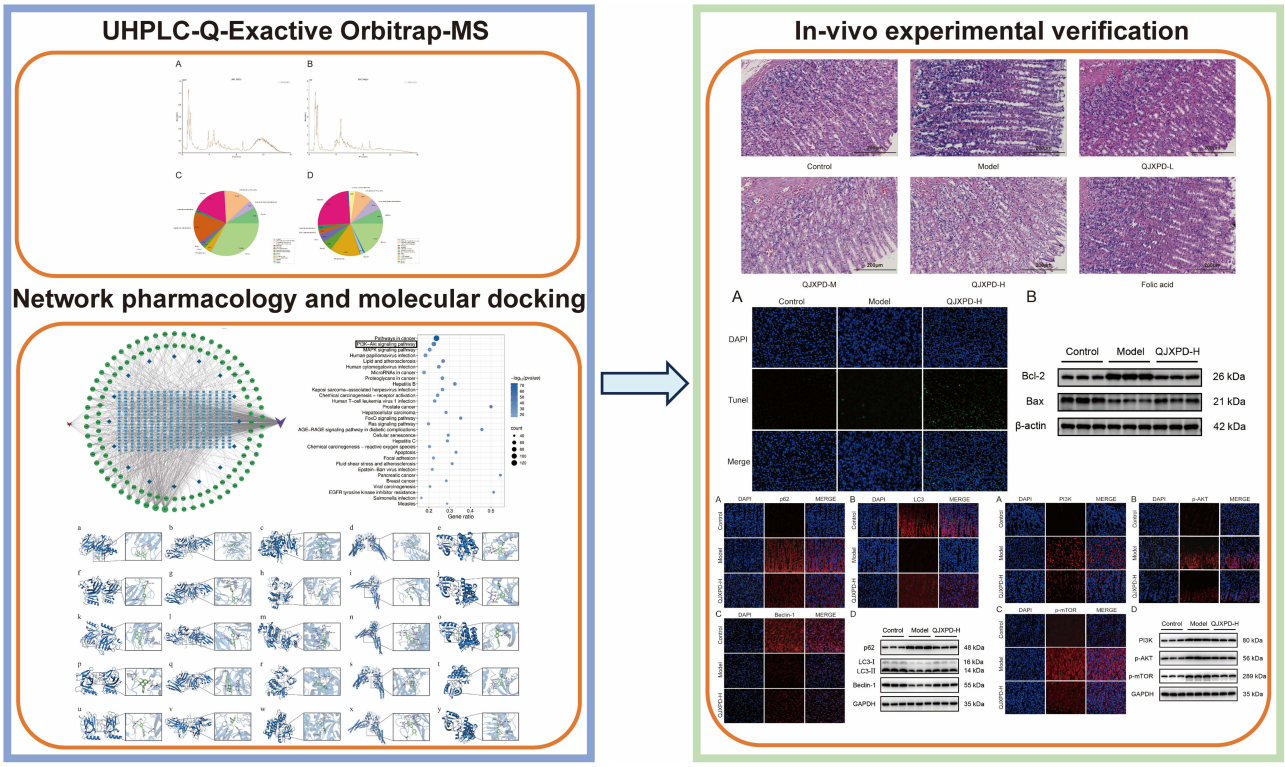

Figure 1 The schematic diagram of this study.

https://doi.org/10.2147/JIR.S532156

Baihuasheshecao 9 g (2310180), Haipiaoxiao 12 g (240126), Zhebeimu 12 g (2401064), Sanqi 10 g (2402085), Dahuang 3 g (2205111), Wumei 10 g (240226), Gancao 6 g (2406157). The Chinese herbal decoction pieces used in this formula were procured from Yongshoutang and Kangtailong Chinese Herbal Decoction Pieces Co., Ltd. Ranitidine hydrochloride (20230215) was obtained from Shanxi Yunpeng Pharmaceutical Group Co., Ltd. (Shanxi, China). N-methyl-N′-nitro -N-nitrosoguanidine (MNNG, M813171) was purchased from Shanghai Macklin Biochemical Co., Ltd. (Shanghai, China). Ammonia water (ST01046) was bought from Hubio (Shenzhen, China). Absolute ethanol (20231223) was obtained from Ningxia Hongyang Chemical (Yinchuan, China). Folic acid tablets (BS945) was purchased from Biosharp (Hefei, China).

Reagents

Methanol (A452-4), acetonitrile (A998-4), and formic acid (A117-50) were purchased from Thermo Fisher Scientific China Co., Ltd. (Massachusetts, USA). Pre-stained Protein Marker (KF002-250) was bought from Shenzhen Sunview Biotechnology Co., Ltd. (Shenzhen, China). PI3K (GTX636838), p-mTOR (GTX132803), p62 (GTX100685), and LC3 (GTX127375) antibodies were purchased from Gene Tex (Texas, USA). p-AKT (YP0006), Beclin-1 (YM1326), Bcl-2 (YM8319), and secondary antibody (RS0002) were obtained from ImmunoWay (California, USA). Bax (50599-2-Ig) antibody was bought from Wuhan Sanying Biotechnology Co., Ltd. (Wuhan, China). TUNEL assay kit (G1504), and antifade mounting medium (G1401) were purchased from Servicebio Biotechnology Co., Ltd. (Wuhan, China). ECL chemiluminescence substrate (KGC460), and total protein extraction kit (KGB5303-50) were obtained from KeyGEN BioTECH Co., Ltd. (Jiangsu, China). Protein Loading Buffer (P1040) was bought from Solarbio Science & Technology Co., Ltd. (Beijing, China). Protein-free rapid blocking buffer (PS108P) was obtained from Epizyme Biomedical Technology Co., Ltd (Shanghai, China).

Equipment

Donatello dehydrator (Diapath, Italy); JB-P5 embedding machine (Wuhan Junjie Electronics Co., Ltd).; RM2016 microtome (Leica, Germany); KD-P tissue flotation bath (Jinhua Kedi Instrument and Equipment Co., Ltd., Zhejiang Province); DS-2S100 decolorization shaker (Wuhan Servicebio Technology Co., Ltd).; Eclipse C1 upright fluorescence microscope (Nikon, Japan); Pannoramic MIDI scanner (3DHISTECH, Hungary); PET 4 mini-vertical electrophoresis transfer tank (Yeasen Biotech Co., Ltd., Shanghai); Amersham Imager 680RGB ultrasensitive multi-functional imager (GE, USA).

Sample Preparation for Identifying Chemical Substances

Preparation of QJXPD

QJXPD was prepared with a compatibility ratio of 15:10:10:10:12:12:12:10:12:9:12:12:10:3:10:6. A 10-fold volume of distilled water was added to the mixture, followed by 2 h soaking and double decoction. The filtrates from both decoctions were combined and subsequently concentrated to a final density of 3.47 g/mL.

Preparation of Sample Solution

The concentrated QJXPD solution was uniformly mixed, and approximately 100 μL was transferred into a centrifuge tube. Subsequently, 900 μL of water (containing 4 μg/mL mixed internal standard) was added, followed by vortex oscillation for 1 min. The tube was then placed in an ice-water bath and subjected to ultrasonic extraction for 60 min, then centrifuged for 10 min. After 5-fold dilution with water, 200 μL of the solution was transferred to an insert-equipped vial for analysis.

UHPLC-Q-Exactive Orbitrap MS/MS Analysis

Instrument and UHPLC-Q-Exactive Orbitrap-MS Conditions

An UHPLC-Q-Exactive Orbitrap analysis was conducted with a liquid chromatography-mass spectrometry setup. It combined an ACQUITY UPLC I - Class plus from Waters (Milford, USA) and a Q-Exactive Orbitrap from Thermo Fisher Scientific (Waltham, MA, USA), operating in Full Scan/Data Dependent (full MS/dd - MS2) acquisition mode.

Chromatographic separation used a Waters ACQUITY UPLC HSS T3 column at 45 °C. A (water with 0.1% formic acid) and B (acetonitrile) served as the mobile phases. The gradient elution program had the following profile: 0–2 min, 5%-5% B; 2–4 min, 5%-30% B; 4–8min, 30%-50% B; 8–10min, 50%-80% B; 10–14 min, 80%-100% B; 14–15 min, 100%-100% B; 15–15.1 min, 100%-5% B; 15.1–16 min, 5% −5% B. The sample injection volume was 5 μL, and the flow rate was 0.35 mL/min. The Q-Exactive Orbitrap MS with a heated electrospray ionization source (HESI) operated in positive and negative ion modes, scanning from m/z 100–1200. The mass spectrometer's operation had these settings: the ion spray voltage was 3000 V for (-)-ESI and 3800 V for (+)-ESI, 320 °C capillary temperature, 350 °C auxiliary gas heater temperature, 35 arb sheath gas flow rate, 8 arb auxiliary gas flow rate, 210–400 nm PDA scan range, and 10, 20, 40 eV collision energies for MS/MS acquisition.

MS Data Preprocessing and Statistical Analysis

Raw LC-MS data were processed using Progenesis QI V3.0 software (Nonlinear, Dynamics, Newcastle, UK), involving baseline filtering, peak identification, integration, retention time correction, peak alignment, and normalization. Key parameters included a 5-ppm tolerance for precursors and 10-ppm for products. Compound identification relied on accurate mass-to-charge ratio (m/z), secondary fragments, and isotope distribution. Qualitative analysis was conducted with The LuMet-TCM (Luming Biotech CO., Ltd, Shanghai, China). Among the substances identified qualitatively in the QI search database, those with a total retention score of 40 or above were chosen as components of the original formula.

Network Pharmacology Analysis

First, the Traditional Chinese Medicine Systems Pharmacology Database (TCMSP, https://old.tcmsp-e.com/tcmsp.php) and High-throughput Chinese Medicine Experiment Reference Database (Herb, http://herb.ac.cn/) were used to search for the active components in QJXPD. The active components retrieved from these databases were intersected with those identified in the original solution via UHPLC-Q-Exactive Orbitrap-MS to determine the key active ingredients of the drug. Subsequently, SwissTargetPrediction (http://www.swisstargetprediction.ch/) was used to predict the targets. Next, Uniprot (https://www.uniprot.org/) was employed to convert target proteins into standard gene names. Disease targets related to PLGC were searched in GeneCards (https://www.genecards.org/) and OMIM (https://www.omim.org) using "Precancerous lesions of gastric cancer" as the keyword. Targets associated with the main ingredients of QJXPD were intersected with the disease targets, and a "Drug-Disease" intersection gene Venn diagram was generated. After that, a "Drug-Ingredient-Target-Disease" network diagram was constructed using Cytoscape V3.10.0 (http://cytoscape.org), followed by visual analysis. The STRING online database V12.0 (https://cn.string-db.org/) was utilized, and data with a confidence level > 0.9 were selected to analyze the "Drug-Disease" intersection genes, yielding a PPI network. Core genes of the network were screened out based on degree. Finally, Gene Ontology (GO) and Kyoto Encyclopedia of Genes and Genomes (KEGG) analyses of the drug-disease intersection targets were conducted via DAVID (https://davidbioinformatics.nih.gov/).

Molecular Docking

The 3D structures of the core genes in the PPI network were retrieved from the Protein Data Bank (PDB) database (https://www.rcsb.org). Water molecules and impurities were removed from the proteins using PyMOL V3.1.0 software. The 3D conformations of the main components of QJXPD were obtained from the PubChem database. AutoDockTools V1.5.6 software was used to hydrogenate the target proteins and small molecules, and a grid box centered on the original ligand was set. Molecular docking between the compound molecules and target proteins was simulated using AutoDock Vina, and the binding energy between the main components and core target proteins was calculated. Finally, the docking results were exported for visual analysis.

In-vivo Experimental Verification

Experimental Grouping and Drug Administration Methods

Using the random number table method, 12 male SD rats were selected from a total of 72 to form the control group, and the remaining 60 rats were designated for establishing the PLGC model. Rats in the control group were fed normally,

while those in the model group were subjected to a five-factor compound modeling method mainly based on MNNG:[26] (1) Free access to MNNG solution: Rats were provided with an MNNG solution (100 μg/mL) for free drinking daily. (2) Abnormal feeding and fasting protocol: Normal feeding for 2 days followed by fasting for 1 day. (3) On fasting days, rats were intragastrically administered 2 mL per rat of 20% anhydrous ethanol (water was withheld 1 hour before and after intragastric administration). (4) On fasting days, the MNNG solution was discontinued, and 0.1% ammonia water was provided for free drinking instead. (5) Chemical drug-induced injury: Rats were intragastrically administered 1 mL/100 g of a 0.003 g/mL ranitidine solution daily. The modeling period lasted for 30 weeks. Twenty-six weeks later, two rats were randomly sampled, and gastric tissues were collected for observation of histopathological changes under a light microscope. Gastric mucosal atrophy, reduced number of proper glands due to inflammatory cell infiltration, intestinal metaplasia, and dysplasia of varying degrees were regarded as indicators of successful establishment of the PLGC model.[27,28] After successful modeling, the rats were allocated into different groups: the model group, folic acid group, and high-dose, medium-dose, and low-dose QJXPD groups, with 12 rats in each group. The QJXPD groups were intragastrically administered 34.65, 17.33, and 8.66 g/kg daily, respectively (the doses were equivalent to 2 times, 1 time, and 0.5 times the dose for a 60 kg adult). The positive control group was intragastrically administered folic acid at a dosage of 0.002 g/kg. Meanwhile, the control group and model group were intragastrically administered an equal volume of physiological saline daily. The intervention lasted for 90 days. After completion of the intervention, the rats were sacrificed and gastric tissues were collected.

Observation of General Conditions

During the experiment, the activity status, fur gloss, fecal characteristics, and body weight of the rats were observed.

HE Staining

The gastric antrum tissues were first subjected to gradient dehydration followed by xylene clearing. Subsequently, paraffin embedding, slicing, and hematoxylin-eosin (HE) staining were carried out. After dehydration and sealing, the alterations in the antral tissues of rats from each group were examined using an optical microscope. Then, a pathological assessment of the rat gastric tissues was performed,[27,28] with the evaluation criteria detailed in Table 1.

TUNEL Staining

Paraffin-embedded antral tissue sections were prepared, and the procedure was then performed rigorously according to the instructions of the TUNEL detection kit. Observations were made using a fluorescence microscope under light-shielding conditions. After staining, apoptotic cells exhibited cyan-green fluorescence. The apoptosis rates of apoptotic cells among various groups were calculated and compared.

Immunofluorescence Colony-Staining

After dewaxing and rehydrating gastric tissue paraffin sections, antigen retrieval was conducted sequentially, followed by washing with PBS. Blocking solution was added to cover the tissue, and blocking was performed at room temperature (RT) in the dark for 30 min. Primary antibodies against the target proteins PI3K, p-AKT, p-mTOR, p62, LC3, and Beclin-1 (1:200) were then added separately, and the sections were placed flat in a moist chamber for incubation at 4°C

Table 1 Histopathological Evaluation Criteria for Precancerous Lesions of Gastric Cancer

Score Calculation	Histopathological Judgment Criteria
0	The structural layers of the gastric mucosa are intact, and no obvious inflammatory changes are observed.
1	The structural layers of the gastric mucosa are basically intact, and inflammatory changes can be observed.
2	The gastric mucosal epithelial layer becomes thinner, the number of glands decreases, mild atrophy, and intestinal metaplasia.
3	The gastric mucosal epithelial layer is thinned or disappeared, with a reduction in the number of glands, moderate atrophy, and intestinal metaplasia.
4	The gastric mucosal epithelial layer disappears, with a decrease in the number of glands, severe atrophy, intestinal metaplasia, or the presence of low-grade intraepithelial neoplasia.

overnight. Next, the specimens were washed with PBS, secondary antibodies were added, and the specimens were incubated in the dark at RT for 50 min. After another PBS wash, DAPI staining solution was added for incubation for 10 min. The sections were mounted with an anti-fluorescence quenching medium, and images were captured using a fluorescence microscope.

Western Blot

For each group of rats, 0.1 g of partial gastric tissue was collected, and total protein was extracted from the gastric tissue. Loading buffer was added, and the mixture was heated in a boiling water bath for denaturation for 10 minutes, then stored at −20°C in a freezer for later use. A polyacrylamide gel was prepared, protein was loaded, electrophoresis was performed, the membrane was transferred, and blocking was then conducted. The membrane was incubated with primary antibodies (1:1000 for Beclin-1 and Bcl-2; 1:2000 for PI3K, p-AKT, p-mTOR, p62, LC3, and Bax) at 4°C overnight. Secondary antibody (1:5000) was then added for incubation at RT for 2 h, followed by the addition of ECL reagent for development. Finally, grayscale analysis was performed using Image J V2.14.0.

Statistical Analysis

Experimental data were analyzed using GraphPad Prism 9.0. Measurement data were presented as mean ± standard deviation (SD). One-way analysis of variance (ANOVA) followed by Tukey's multiple comparisons test was used to compare the data involving multiple group comparisons. $P<0.05$ was regarded as statistically significant.

Results

Identification of Components of QJXPD

QJXPD was analyzed by LC-MS, and the compounds were preliminarily identified. Figure 2A and B shows the UHPLC-MS chromatograms of QJXPD in positive and negative ion modes. We made a comparison between QJXPD and the standard substance database (LuMet-TCM). According to the precise mass-to-charge ratio (m/z), secondary fragments, and isotope distribution, 1069 ingredients in QJXPD were recognized, including flavonoids, terpenoids, phenols, sugars and glycosides, alkaloids, and other compounds. The content and quantity distribution of its component classification are shown in Figure 2C and D.

Network Pharmacological Analysis

A total of 945 active ingredients were acquired through database searches. After intersecting these with the identified components of the original solution, 119 key ingredients and 398 targets of active ingredients were determined. When searching the GeneCards and OMIM databases, 2027 potential biomarkers associated with PLGC were retrieved. Subsequently, through intersection analysis, 332 potential targets were identified as common to both the targets corresponding to the active ingredients of the drug and the disease-related proteins (Figure 3A). PPI network showed core targets, including TP53, AKT1, SRC, STAT3, and EGFR (Figure 3B). Drug-compound-common targe-disease network to illustrate the relationship between active ingredients and their corresponding targets in drugs (Figure 3C). From the GO enrichment analysis, 832 GO terms were obtained (Figure 4A). In the BP terms, they were mainly focused on positive regulation of transcription by RNA polymerase II, signal transduction, and negative regulation of the apoptotic process. The CC terms were mainly concentrated in the cytosol, cytoplasm, and nucleus. The MF terms were mainly related to protein binding, identical protein binding, and ATP binding. The KEGG pathway enrichment analysis screened out 179 pathways related to PLGC. These chiefly encompassed pathways in cancer, the PI3K-AKT pathway, and the MAPK pathway (Figure 4B).

Main Active Ingredients of QJXPD

Among the components through which QJXPD exerts its therapeutic effects, the top five active ingredients were identified as Quercetin, Resveratrol, Genistein, Kaempferol, and Luteolin, based on their degree values. The chemical details of these five ingredients are presented in Table 2.

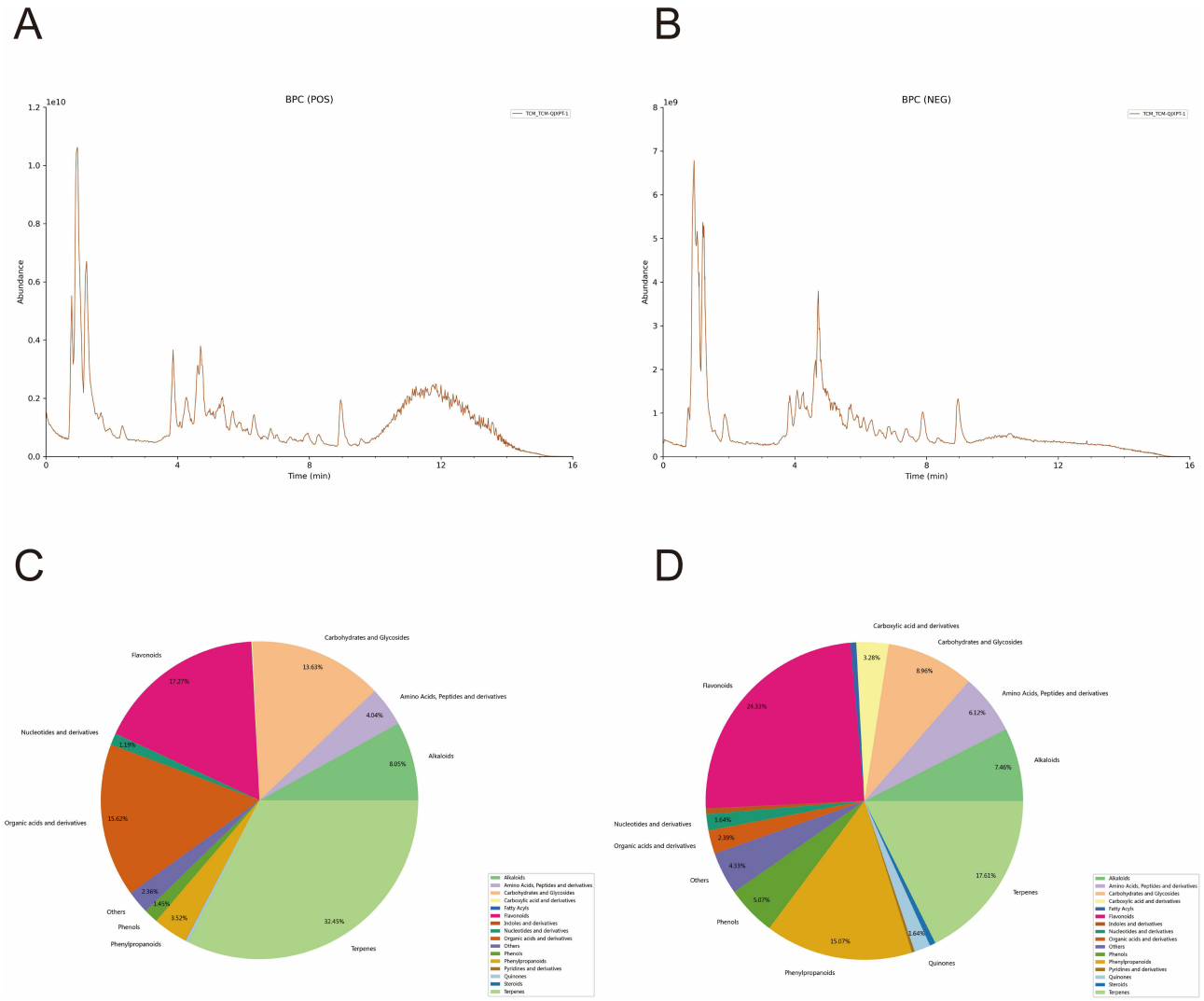

Figure 2 Chromatogram and Component Classification Diagram of QJXPD. (**A**) Positive total ion chromatogram of QJXPD; (**B**) Negative total ion chromatogram of QJXPD; (**C**) Distribution diagram of component classification content of QJXPD; (**D**) Distribution diagram of the quantity of component classification of QJXPD.

Molecular Docking Results

The docking results showed that Quercetin, Resveratrol, Genistein, Kaempferol, and Luteolin have good binding energies with TP53, AKT1, SRC, STAT3, and EGFR, the docking score and 3D pattern diagrams were displayed in Figure 5A and B.

QJXPD Improves the General Condition and Gastric Mucosal Tissue Pathological Changes in PLGC Rats

QJXPD has a notable impact on the growth and development of rats. In the control group, rats exhibit a good mental state, with normal activities. Their fur is soft and smooth, reactions are rapid and sensitive, and stools are well-formed. The rats in the model group show lethargy, slow reactions, squinting, drowsiness, fatigue, laziness, loose and soft stools, and dull and dry fur. After drug intervention, the general condition of rats in each drug-administered group improved compared to the model group. The model group had significantly lower body mass than the control group ($P<0.01$). In contrast, TCM groups and the folic acid group showed significantly increased body mass compared to the model group ($P<0.01$), indicating QJXPD can improve PLGC rats' general condition (Figure 6A). Pathological scoring showed that (Figure 6B and C), the model group had a significantly higher score than the control group ($P<0.01$), while the high-dose QJXPD group had a significantly lower score than the model group ($P<0.01$). HE staining was employed to evaluate

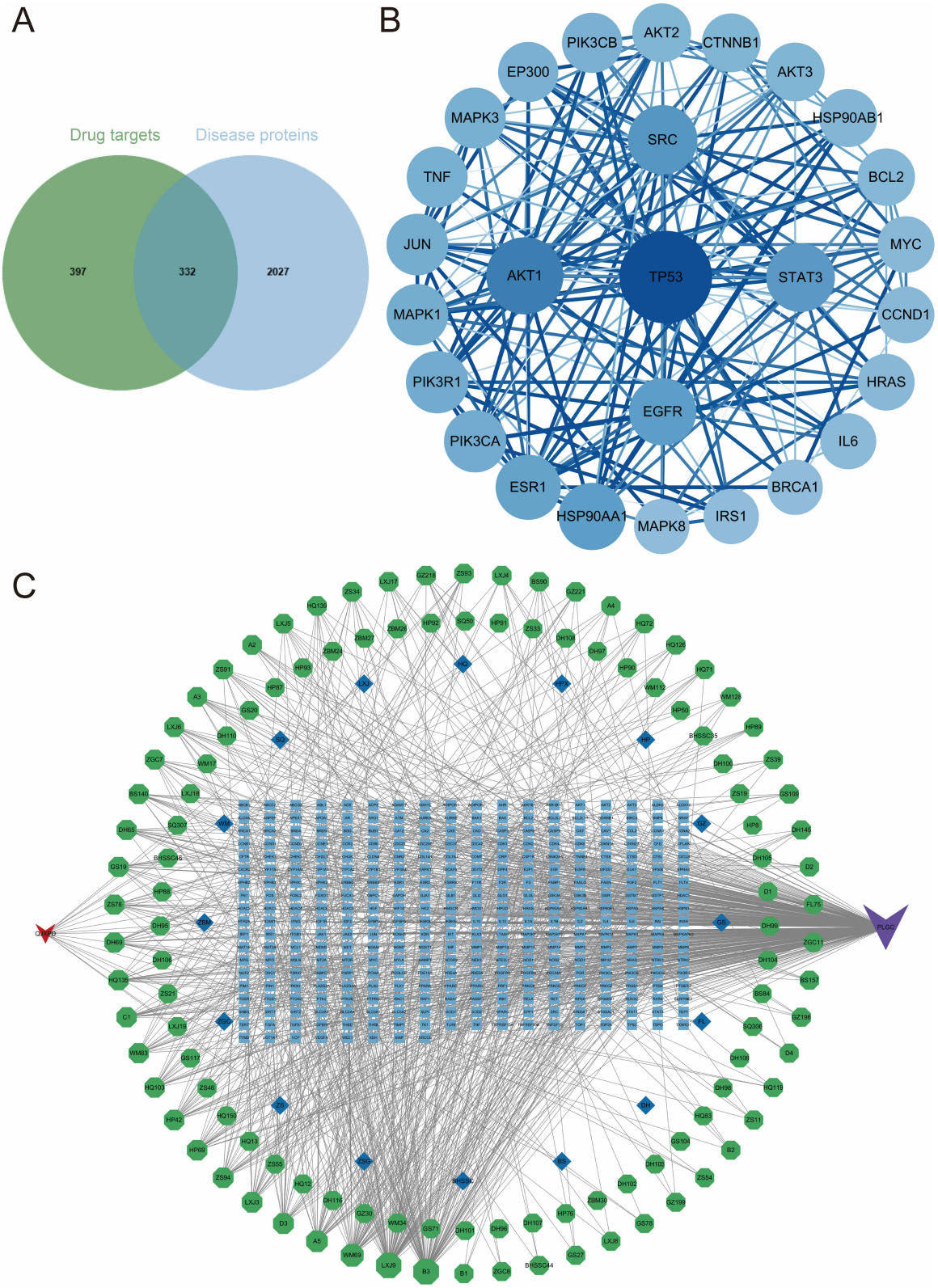

Figure 3 Common targets for QJXPD and PLGC, core targets, and drug-disease-compound-common target network. (**A**) Venn diagram of common targets for QJXPD genes and PLGC proteins. (**B**) Core targets were chosen based on degree values. The larger size of a node represented a higher value of degree. The deeper color represented the more importance in the PPI network. (**C**) Drug-compound-common targe-disease network. The light blue nodes represented the common targets for QJXPD genes and PLGC proteins, the dark blue nodes represent the drug composition of QJXPD, whereas the green nodes represented common compounds for QJXPD and PLGC.

Abbreviations: B3, Quercetin; LXJ9, Resveratrol; WM69, Genistein; A5, Kaempferol; D3, Luteolin.

https://doi.org/10.2147/JIR.S532156

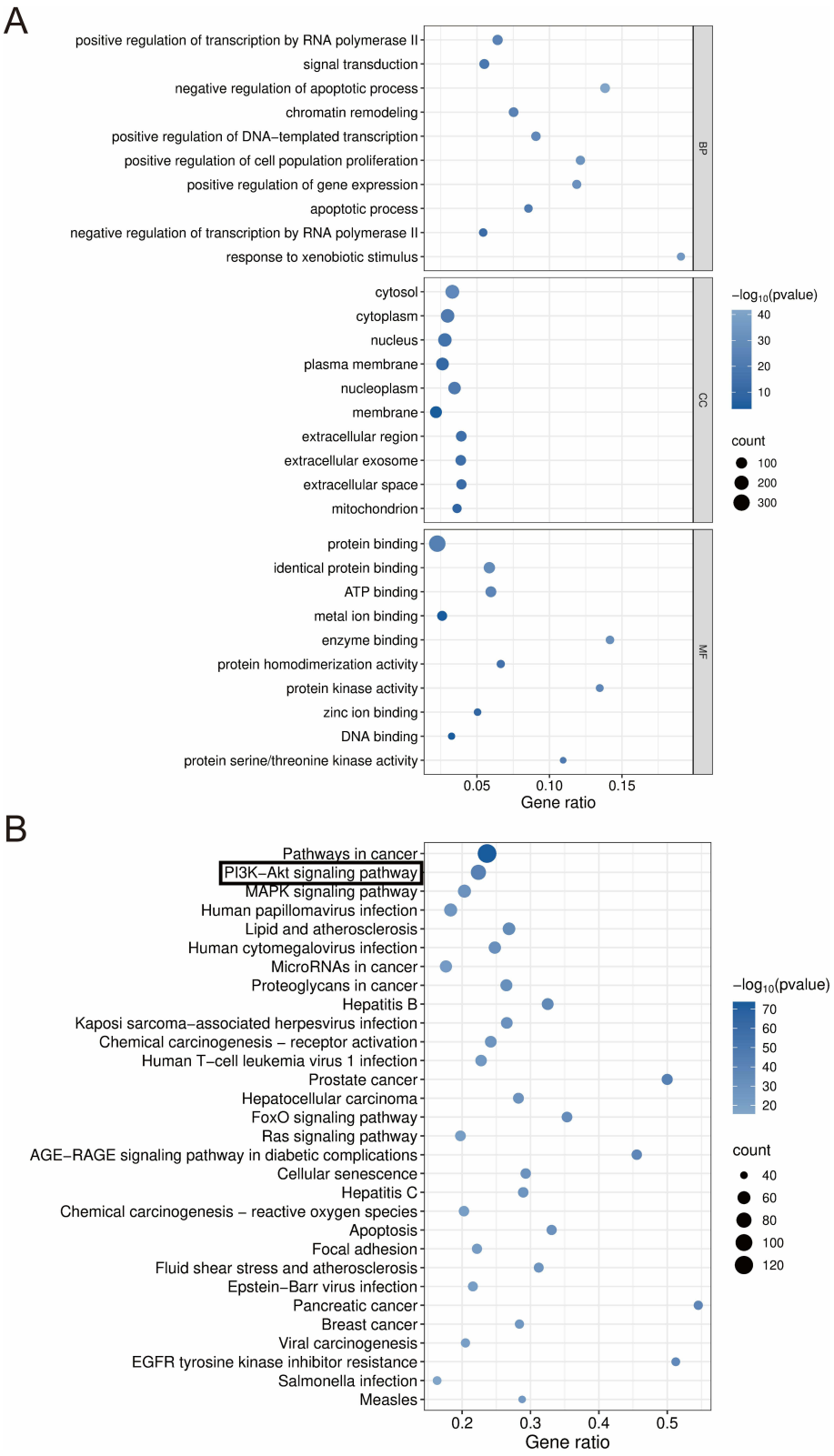

Figure 4 Enrichment analysis of the GO and KEGG pathways of potential targets. (**A**) A bar chart presents the top 30 results from GO enrichment analyses, categorized by Biological Process (BP), Cellular Component (CC), and Molecular Function (MF). The length of each bar corresponds to the number of genes, while the color indicates the *P*-value threshold for the enrichment of potential targets within the Gene Ontology. (**B**) The top 30 pathways enriched by the KEGG pathway. The x axis shows the gene ratio. In the graph, the size of the bubbles represents the number of genes, and the color represents the *P*-value.

Table 2 Identification of the Chemical Constituents of QJXPD

No	RT (min)	M/Z	Formula	Adducts	Mode	Compounds	Source
1	4.56	627.1548	$C_{15}H_{10}O_7$	M+H	POS	Quercetin	Huangqi, Sanqi, Wumei
2	5.65	246.1121	$C_{14}H_{12}O_3$	M+NH_4	POS	Resveratrol	Longxuejie
3	6.89	271.0595	$C_{15}H_{10}O_5$	M+H	POS	Genistein	Wumei
4	7.02	285.0402	$C_{15}H_{10}O_6$	M-H	NEG	Kaempferol	Huangqi, Baishao, Wumei
5	6.17	285.0404	$C_{15}H_{10}O_6$	M-H	NEG	Luteolin	Zhishi, Guizhi

gastric mucosal lesions (Figure 6D). In the control group, gastric mucosa was intact with normal epithelium, orderly glands, no dilation, and no inflammation. The model group had severely thinned mucosa, deformed and fewer glands, dilated cavities, and abundant inflammation. The folic acid group had relatively thin mucosa, fewer and less-orderly cells and glands, and more inflammation in parts. Compared with the model group, the low, medium, and high-dose QJXPD groups showed graded mucosal repair, with more and better-arranged glands and less inflammation. This indicates QJXPD protects PLGC rats' gastric mucosa, with the high-dose showing the best efficacy.

QJXPD Activates Autophagy in Gastric Mucosal Cells of PLGC Rats

IFC enables the detection of target-protein localization and expression in tissues (Figure 7A–D). We applied it to detect autophagy-related protein expression in the antral tissue of PLGC rats. Compared with the control group, the expression of p62 protein in the antral tissue of rats in the model group was elevated ($P<0.01$), while the expression of LC3 and Beclin-1 proteins was reduced ($P<0.01$). Compared with the model group, the expression of p62 protein in the high-dose QJXPD group was decreased ($P<0.01$), and the expression of LC3 and Beclin-1 proteins was increased ($P<0.01$). Western blot analysis revealed that (Figure 7E and F), when compared to the control group, the expression of p62 protein in the gastric tissue of rats in the model group was increased ($P<0.01$), while the expression of LC3 and Beclin-1 proteins was decreased ($P<0.01$). In comparison with the model group, the expression of p62 protein in the high-dose QJXPD group was decreased ($P<0.01$), and the expression of LC3 and Beclin-1 proteins was increased ($P<0.01$). Results from both experiments demonstrated that QJXPD could activate autophagy in gastric mucosal cells of PLGC rats.

QJXPD Induces Gastric Mucosal Cell Apoptosis in PLGC Rats

The TUNEL staining method was employed to assess the cell apoptosis status (Figure 8A and B). Results demonstrated that the apoptosis rate of antral tissue cells in the high-dose QJXPD group was higher than that in the model group ($P<0.01$), suggesting that QJXPD can promote apoptosis of gastric mucosal cells in PLGC rats. Western blot was applied to detect the changes in apoptosis-related proteins (Figure 8C and D). Compared with the control group, the expression of Bcl-2 protein in the gastric tissue of rats in the model group was upregulated ($P<0.01$), while the expression of Bax protein was downregulated ($P<0.01$). Compared with the model group, the expression of Bcl-2 protein in the QJXPD high-dose group was decreased ($P<0.01$), and the expression of Bax protein was increased ($P<0.01$). Both experimental approaches consistently demonstrated that QJXPD induces apoptosis of gastric mucosal cells in PLGC rats.

QJXPD Inhibits the Activation of the PI3K/AKT/mTOR Pathway

PI3K and AKT can affect various biological processes, including tumor cell proliferation, apoptosis, angiogenesis, and metabolism. mTOR is a crucial regulator in the autophagy initiation stage, which can negatively regulate the occurrence of autophagy.[29–31] To elucidate the mechanism of QJXPD in treating PLGC rats, we analyzed the PI3K/AKT/mTOR pathway. IFC results indicated that (Figure 9A–D), compared with the control group, the expression of PI3K, p-AKT, and p-mTOR proteins in the gastric tissue of rats in the model group was upregulated ($P<0.01$); compared with the model group, the expression of PI3K, p-AKT, and p-mTOR proteins in the QJXPD high-dose group was downregulated ($P<0.01$). Western blot analysis further corroborated these findings (Figure 9E and F). Similar to the IFC results, the expression of PI3K, p-AKT, and p-mTOR proteins in the model group was notably increased compared with the control group ($P<0.01$). And when compared

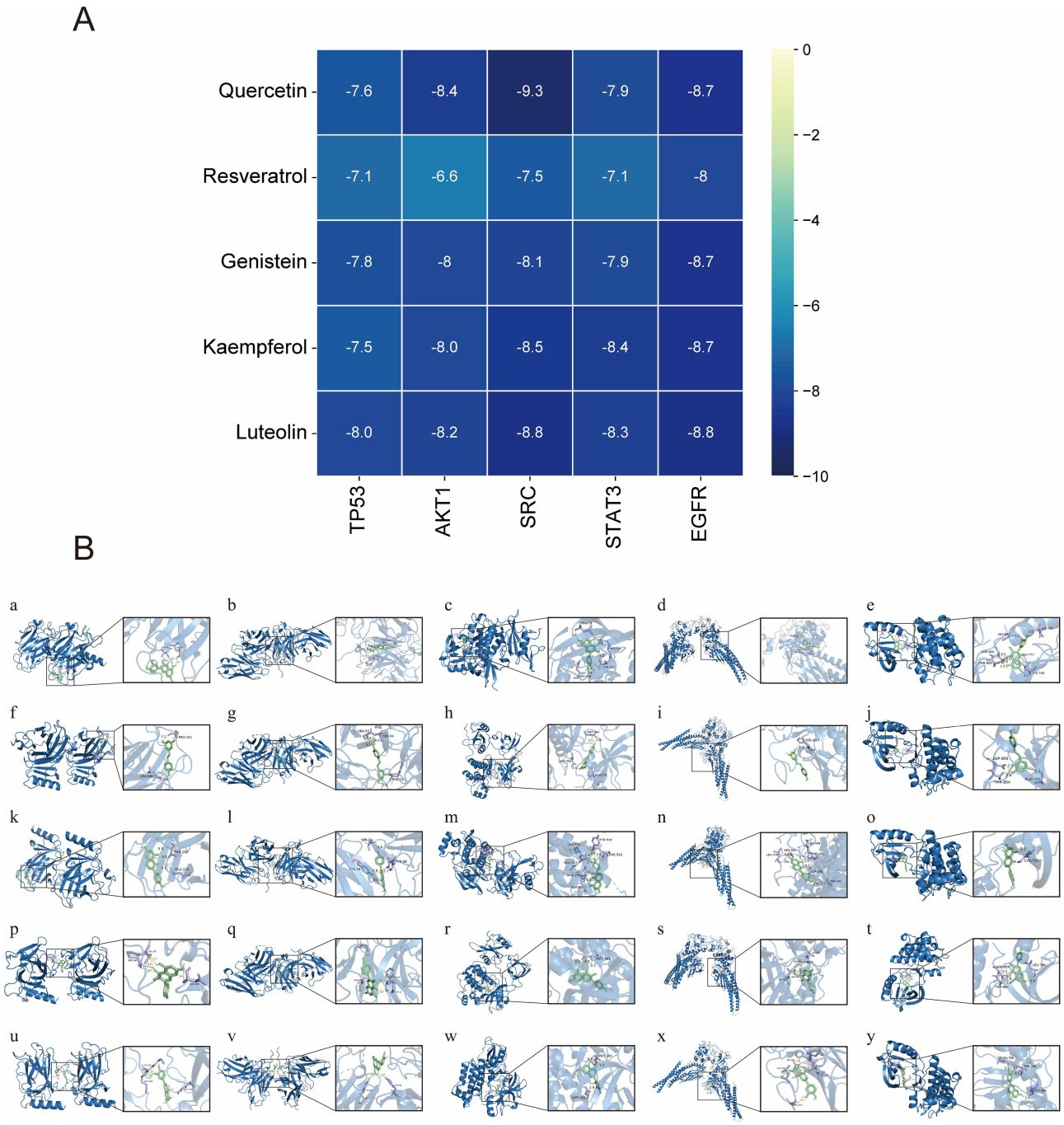

Figure 5 Molecular docking heat maps and models that pair the top 5 main ingredients with the top 5 core targets. (**A**) The binding energy (kcal/mol) between the main ingredients and the core targets. (**B**) Molecular Docking 3D Diagrams of main ingredients with the core targets. a~e: Quercetin docking TP53, AKT1, SRC, STAT3, EGFR; f~j: Resveratrol docking TP53, AKT1, SRC, STAT3, EGFR; k~o: Genistein docking TP53, AKT1, SRC, STAT3, EGFR; p~t: Kaempferol docking TP53, AKT1, SRC, STAT3, EGFR; u~y: Luteolin docking TP53, AKT1, SRC, STAT3, EGFR.

with the model group, the expression of these proteins in the high-dose QJXPD group was notably decreased (P<0.01). Findings from the two experiments indicated that QJXPD suppresses the activation of the PI3K/AKT/mTOR pathway.

Discussion

Epidemiological studies[32] indicated a link between CAG development and the long-term consumption of carcinogens such as nitrite. MNNG is a strong nitrite mutagen, the histological characteristics of GC induced by it are similar to those

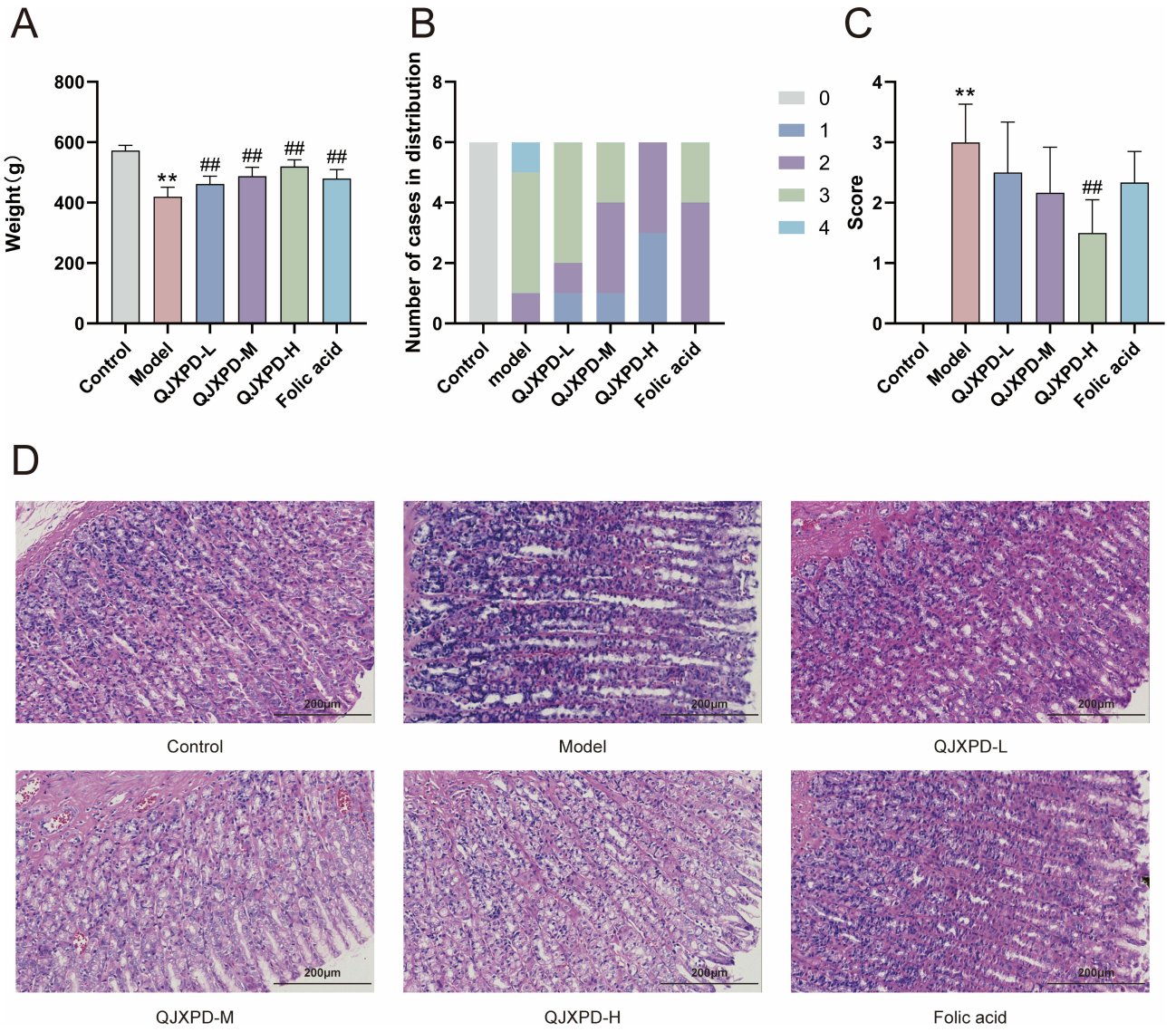

Figure 6 Changes in body weight and histopathological alterations of the gastric mucosa in rats. (**A**) Changes in body weight of rats in each group at the end of treatment. (**B** and **C**) Effect of QJXPD on the graded distribution and quantitative score of the degree of gastric mucosal lesions in the PLGC rat model (n=6). (**D**) Histopathological Changes of the Gastric Mucosa in Various Groups (HE staining, Bar=200μm). Compared to the control group, $^{**}P$ <0.01; Compared to the model group, $^{\#\#}P$ <0.01.

of human GC.[33] It is commonly used to replicate animal models of CAG, PLGC, and GC,[34] long-term low-concentration intake of MNNG combined with abnormal satiety can increase the probability of successfully replicating PLGC animal models,[35] resulting in different degrees of pathological manifestation.[36] Meanwhile, as PLGC result from the combined action of multiple factors and requires a long-term process, when using MNNG to establish a PLGC rat model, it is often combined with other factors.[37] Liang Guoying et al[38] also successfully established a PLGC rat model after 16 weeks of combined modeling using the method of free drinking of MNNG solution, irregular feeding patterns, and intragastric administration of sodium deoxycholate and ethanol. In this experiment, the combined method employed was allowing the rats to freely drink a 100 μg/mL MNNG solution along with a 0.003 g/mL ranitidine solution. The feeding pattern was to feed for 2 days and then fast for 1 day. On the fasting days, rats were given 20% absolute ethanol via intragastric administration, and they were also allowed to freely drink 0.1% ammonia water. After 26 weeks, compared with the control-group rats, the gastric mucosa of the antrum tissue in the model group was notably thinner, the glands were deformed, decreased in number, and disorderly arranged, the glandular lumens were obviously dilated, and has substantial inflammatory cell infiltrations. Moreover, the pathological scores of the rat gastric tissues increased

https://doi.org/10.2147/JIR.S532156

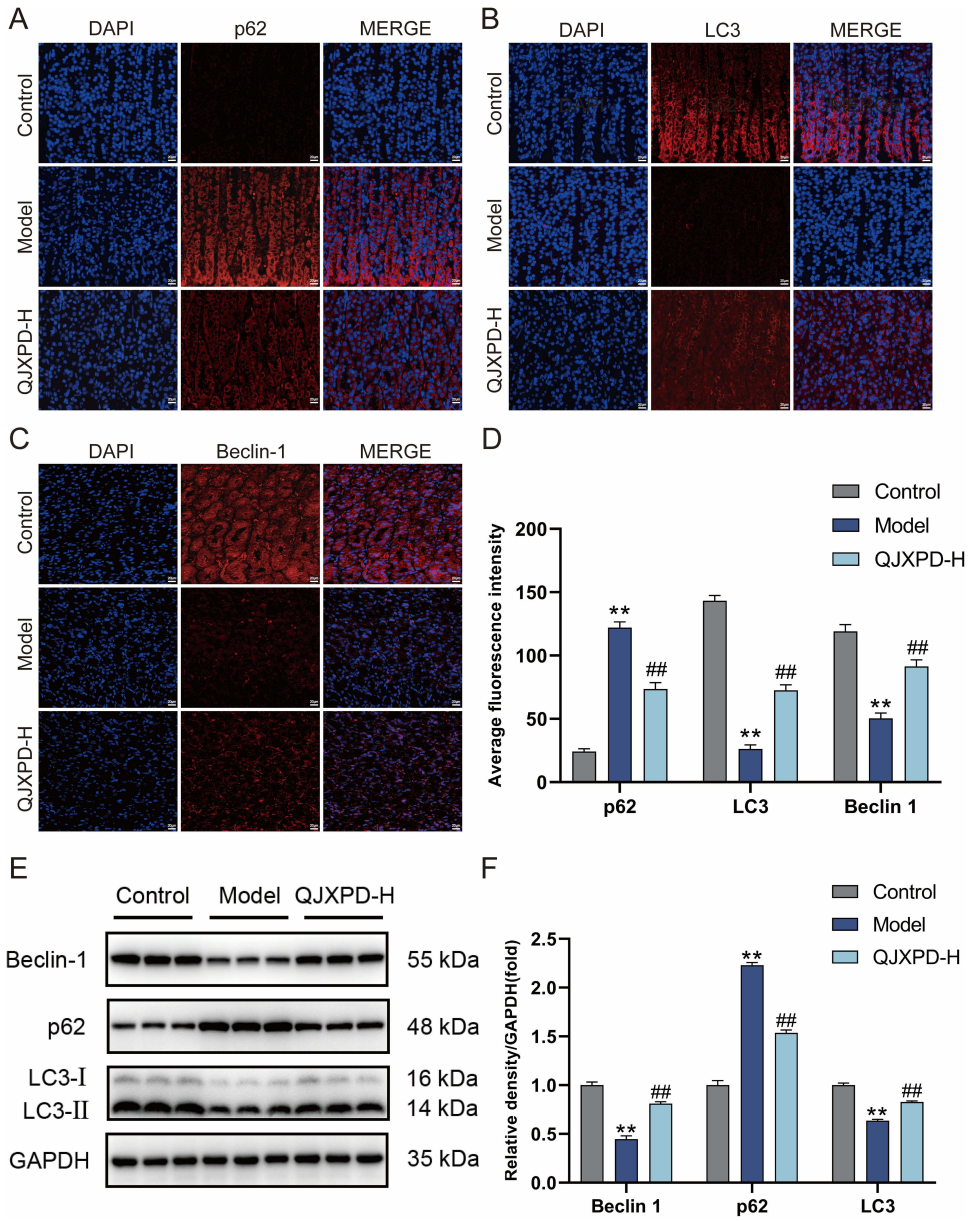

Figure 7 QJXPD activates autophagy in gastric mucosal cells of PLGC rats. (**A~C**) IFC to detect the impact of QJXPD on the expression of p62, LC3, and Beclin-1 proteins in gastric sinus tissues of PLGC rats. (**D**) Average fluorescence intensity of p62, LC3, and Beclin-1 analyzed by IFC. (**E**) Effect of QJXPD on p62, LC3, and Beclin-1 protein expression in gastric sinus tissue of PLGC rats detected by Western Blot. (**F**) Protein expression of p62, LC3, and Beclin-1 analyzed by Western blotting. n=3-6. Compared to the control group, $^{**}P$ <0.01; Compared to the model group, $^{\#\#}P$ <0.01.

significantly, indicating the successful induction of the PLGC model. Through the intervention of QJXPD, the body weight of the PLGC model rats increased, the pathological conditions of the gastric mucosa improved, and the pathological scores declined. These findings imply that QJXPD has a significant therapeutic impact on PLGC rats.

QJXPD is an effective prescription for the treatment of PLGC. Previous studies conducted by our research team have also confirmed the safety of QJXPD. In this research, we elucidate the chemical components of QJXPD through UHPLC-Q-Exactive Orbitrap-MS. In comparison with positive standards, 1069 compounds were recognized in QJXPD, encompassing flavonoids, terpenoids, phenols, sugars and glycosides, alkaloids, and other compounds. Most of these compounds have the function of regulating autophagic cell death, which is an important way to achieve its anti-tumor efficacy.[39] After network pharmacology analysis, we predicted that 119 active ingredients and 332 potential targets were capable of ameliorating PLGC. The main ingredients included quercetin, resveratrol, genistein, kaempferol, and luteolin.

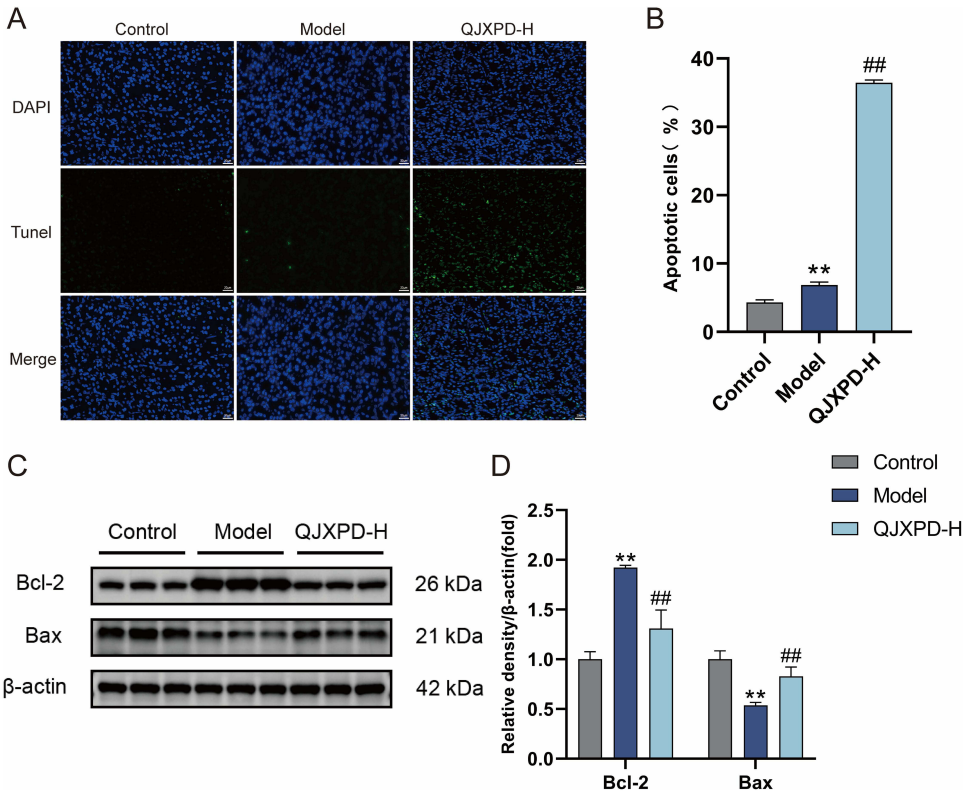

Figure 8 QJXPD promotes apoptosis of gastric mucosal cells in PLGC rats. (**A**) TUNEL method to detect apoptosis. (**B**) Cell apoptosis analysis using the TUNEL method. (**C**) Western Blot to detect the effect of QJXPD on the expression of Bax and Bcl-2 proteins in the gastric sinus tissue of PLGC rats. (**D**) Protein expression of Bax and Bcl-2 analyzed by Western blotting. n=3-6. Compared to the control group, $^{**}P$ <0.01; Compared to the model group, $^{\#\#}P$ <0.01.

Quercetin can activate and up-regulate the expression of the p53 gene, suppress the proliferation and migration ability of GC cells, and alleviate inflammatory damage to the gastric mucosa,[40,41] and it has been proven to have anti-cancer activities related to apoptosis and autophagy induction.[42] Resveratrol can prevent and treat the occurrence and progression of GC by promoting tumor cell apoptosis while suppressing their proliferation, invasion, and migration.[43–45] Genistein exerts a potent inhibitory impact on the proliferation of GC cells and can induce their apoptosis.[46] Kaempferol can lower the expression of inflammatory factors in the gastric mucosa of rats with PLGC, thereby delaying the progression of the disease.[47] Luteolin can alleviate the degree of gastric mucosal inflammation and the extent of damage in PLGC rats,[48] effectively halt the progression of GC.[49] These findings suggesting that the effective components of QJXPD exert synergistic effects, QJXPD may be an effective drug for treating or reversing PLGC, and further highlights the great significance of exploring the underlying mechanism of QJXPD in PLGC treatment.

The key targets of QJXPD in treating PLGC include TP53, AKT1, SRC, STAT3, and EGFR. TP53 serves is a crucial tumor-suppressor gene, studies have found that there is a certain correlation between gastric mucosal injury and changes in TP53 expression,[50] and TP53 gradually increases during the "inflammation-cancer" transformation process, with the strongest expression in GC.[51] This gene plays a significant role in regulating autophagy, when encountering stressors such as a lack of nutrients or low-oxygen (hypoxic) environments, TP53 can induce autophagy, it achieves this induction by suppressing the mTOR signaling route.[52] AKT1 exhibits a high expression state in the PLGC and the GC stage,[12] many TCM monomers can suppress the proliferation, invasion and migration of GC cells and stimulate cell apoptosis and autophagy through the PI3K/AKT pathway.[53] SRC protein demonstrates a high-level expression in GC tissues, when the expression of the SRC protein is inhibited, it can curtail the proliferation of GC cells and facilitate apoptosis.[54] STAT3 assumes a crucial role in the advancement of GC, high-level expression of the STAT3 gene favors the survival of GC cells, and phosphorylated STAT3 can further promote the proliferation of GC cells.[55,56] EGFR abnormal overexpression is strongly associated with GC pathogenesis and its precancerous stages, its expression rises as gastric mucosa progresses

https://doi.org/10.2147/JIR.S532156

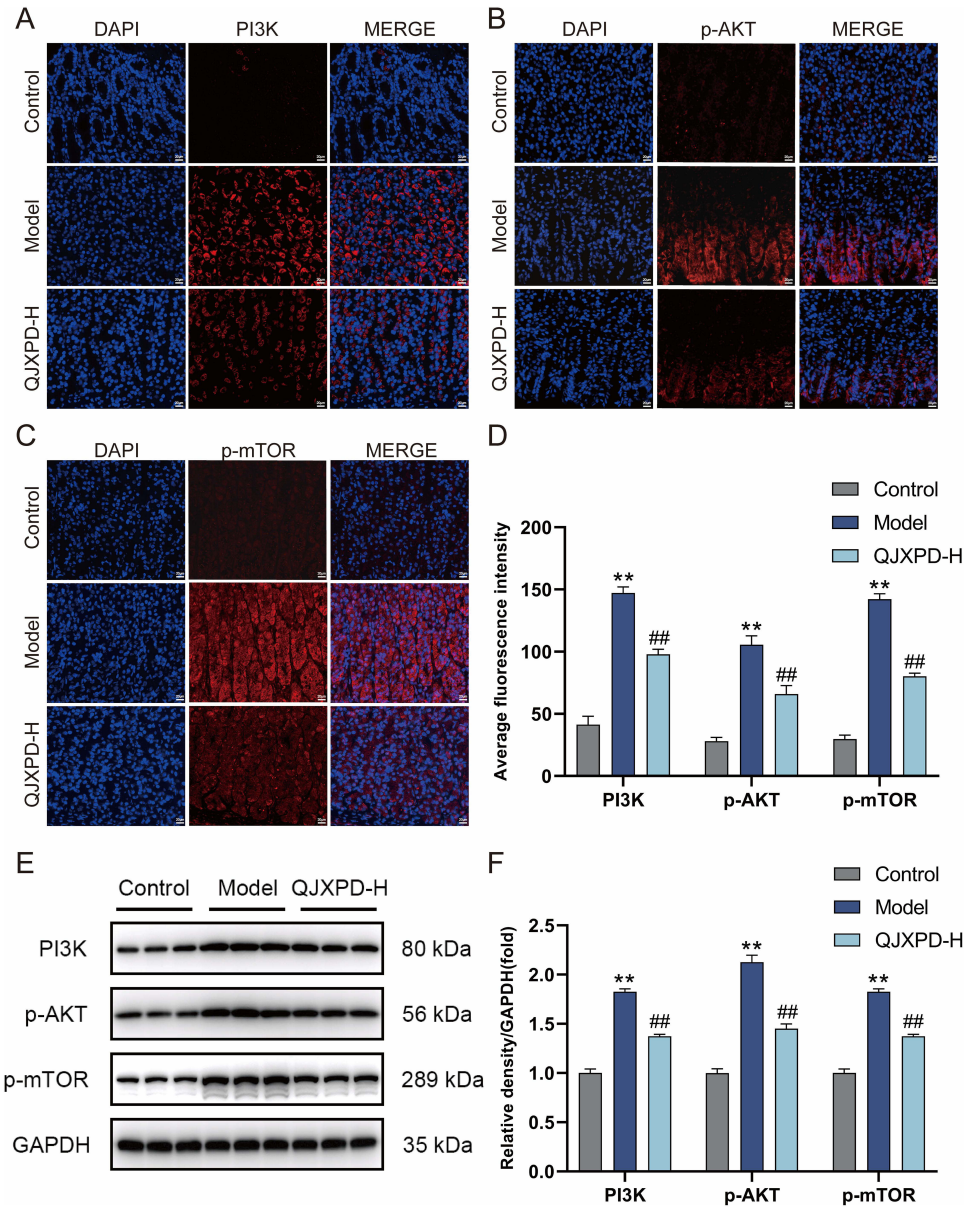

Figure 9 QJXPD inhibits the activation of PI3K/AKT/mTOR signaling pathway. (**A~C**) IFC to detect the impact of QJXPD on the expression of PI3K, p-AKT, and p-mTOR proteins in gastric sinus tissues of PLGC rats. (**D**) Average fluorescence intensity of PI3K, p-AKT, and p-mTOR analyzed by IFC. (**E**) Effect of QJXPD on PI3K, p-AKT, p-mTOR protein expression in gastric sinus tissues of PLGC rats detected by Western blotting. (**F**) Protein expression of PI3K, p-AKT, and p-mTOR analyzed by Western blotting. n=3-6. Compared to the control group, $^{**}P$ <0.01; Compared to the model group, $^{\#\#}P$ <0.01.

from chronic inflammation to GC. Research has shown that the EGFR/PI3K/AKT pathway is abnormally activated in a rat model of PLGC, inhibition of this pathway has been shown to effectively ameliorate PLGC.[57] Evidently, QJXPD might influence the onset and progression of PLGC through the regulation of the key targets mentioned above.

The findings from the KEGG enrichment analysis indicated that QJXPD can ameliorate PLGC via diverse pathways, including the PI3K/AKT and the MAPK pathway. Collectively, the aforementioned data suggest that QJXPD acts on PLGC via multiple ingredients, targets, and pathways. Integrating the key targets, enrichment pathway analysis, and a comprehensive review of relevant literature, we conducted subsequent experimental validation regarding the involvement of the PI3K/AKT/mTOR pathway. It should be emphasized that the outcomes of molecular docking revealed that the principal active ingredients of QJXPD exhibit favorable binding affinity to the key targets. Moreover, in-vivo

experiments demonstrated that QJXPD can mitigate PLGC. It achieves this by triggering autophagy and apoptosis through the inhibition of the PI3K/AKT/mTOR pathway.

Autophagy and apoptosis are both interconnected and distinct from each other, and serve as crucial biological processes in the initiation and progression of GC. Studies have shown that the level of autophagy is inhibited during the PLGC stage, especially when dysplasia occurs.[58,59] Therefore, promoting autophagy is an important approach for treating mild to severe PLGC. In the CAG stage, excessive apoptosis of gastric mucosal epithelial cells leads to mucosal atrophy changes, while in the dysplasia stage, apoptosis disorders occur and proliferation continues to increase, thereby triggering hyperplasia.[60] The PI3K/AKT/mTOR pathway is a crucial route for regulating cell autophagy and apoptosis.[61] Under physiological conditions, PI3K can convert phosphatidylinositol bisphosphate into phosphatidylinositol trisphosphate, bind to AKT and phosphorylate it, and p-AKT upregulates mTOR expression, thereby inhibiting cell autophagy.[62] This pathway can also suppress cell survival by regulating apoptosis-related genes such as Bax and Bcl-2.[63] Studies have shown that by inhibiting the PI3K/AKT/mTOR pathway, cell apoptosis and autophagy can be regulated, thus offering a protective function against gastric mucosal damage in PLGC.[25] Evidently, the PI3K/AKT/mTOR pathway is tightly linked to the state and function of cells. Studies have confirmed[64] that the PI3K/AKT/mTOR pathway is activated in the gastric tissues of rats with precancerous gastric lesions and in gastric cancer cells. TCM can induce protective cell autophagy by suppressing the PI3K/Akt/mTOR pathway, thereby delaying the onset and development of GC. In this study, the expression of PI3K, p-AKT, p-mTOR, p62 and Bcl-2 proteins in the antral tissue of PLGC model rats was notably elevated, while the expression of Beclin-1, LC3 and Bax proteins was significantly decreased. This indicates that the PI3K/AKT/mTOR pathway was dysregulated and cellular autophagy and apoptosis are inhibited. After intervention with QJXPD, the expression of PI3K, p-AKT, p-mTOR, p62 and Bcl-2 proteins was significantly lowered, and the expression of Beclin-1, LC3 and Bax proteins was notably increased, and the cells in the gastric antrum tissue show a higher apoptosis rate. This suggests that QJXPD may activate cell autophagy and promote cell apoptosis by suppressing the PI3K/AKT/mTOR pathway, thus achieving the purpose of treating PLGC (Figure 10).

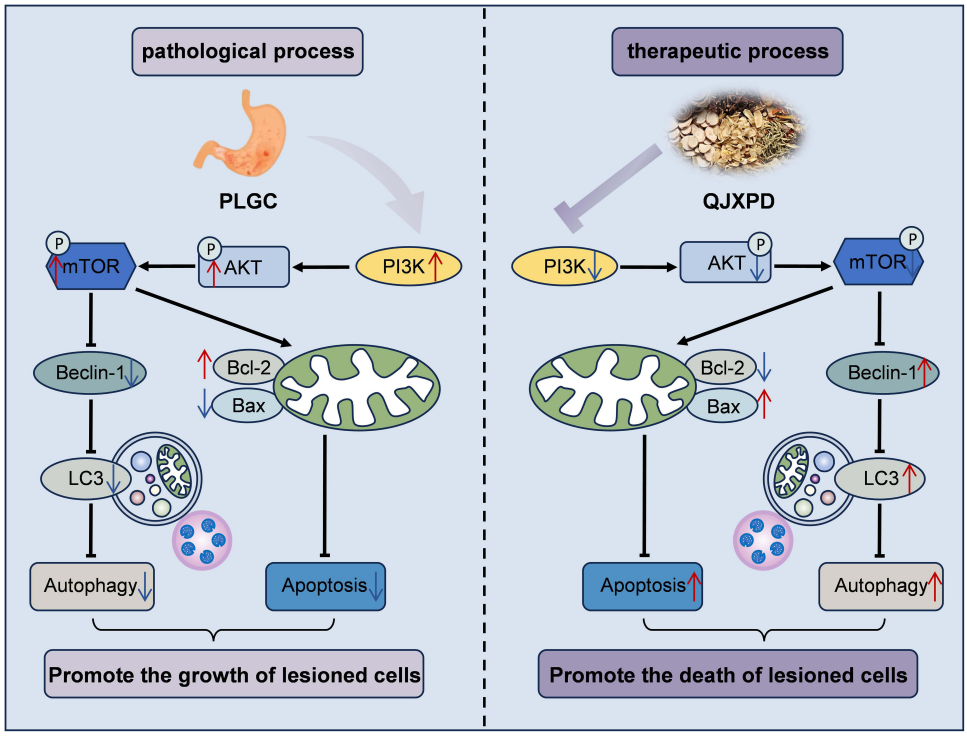

Figure 10 The mechanism of action of QJXPD in treating PLGC.

https://doi.org/10.2147/JIR.S532156

Conclusion

This study combined UHPLC-Q-Exactive Orbitrap-MS, network pharmacology, molecular Docking, and experimental verification to uncover the possible mechanism of action of QJXPD in treating PLGC. By replicating the PLGC rat model, it was verified that QJXPD may alleviate the gastric mucosal pathological damage in PLGC rats by suppressing the PI3K/AKT/mTOR pathway estimated by network pharmacology, promoting cell autophagy and apoptosis. This provides an experimental foundation for the clinical management of GC and PLGC. Nevertheless, this study has certain limitations, for instance, the interrelationship between autophagy and apoptosis still needs to be elucidated, which will be one of the focuses of future research.

Abbreviations

QJXPD, Qijie Xiaopi Decoction; PLGC, Precancerous lesions of gastric cancer; UHPLC-Q-Exactive Orbitrap-MS, Ultra-high-performance liquid chromatography coupled with hybrid quadrupole-orbitrap tandem mass spectrometry; PI3K, Phosphatidylinositol 3-kinase; AKT, Protein kinase b; mTOR, Mammalian target of rapamycin; MNNG, N-methyl-N'-nitro-N-soguanidine; LC3, microtubule-associated protein light chain 3; p62, Sequestosome 1; Bax, Bcl-2-associated X; Bcl-2, B-cell lymphoma 2; HE, Hematoxylin-eosin.

Data Sharing Statement

Data sets used and/or analyzed during the current study period are available from the corresponding author, Junrui Hu, upon reasonable request.

Ethics Approval

The animal study was approved by Animal Ethics Committee of Ningxia Medical University (IACUC-NYLAC-2023-198). The animal experiments were conducted in accordance with the Guide for the Care and Use of Laboratory Animals published by the National Research Council (NRC).

Consent for Publication

All authors critically reviewed the content of the manuscript. The consent for publication was obtained from all authors.

Author Contributions

All authors contributed to data analysis, drafting or revising the article, have agreed on the journal to which the article will be submitted, gave final approval of the version to be published, and agree to be accountable for all aspects of the work.

Funding

This study was supported by the Key Research and Development Program of Ningxia Hui Autonomous Region (2022BEG03150) and the Research Plan of the Scientific Research Funding Project of Ningxia Medical University (XZ2022006).

Disclosure

The authors report no conflicts of interest in this work.

References

1. Xia C, Dong X, Li H, et al. Cancer statistics in China and United States, 2022: profiles, trends, and determinants. *Chinese Med J*. 2022;135(5):584–590. doi:10.1097/CM9.0000000000002108
2. Hatakeyama M. Helicobacter pylori and gastric carcinogenesis. *J Gastroenterol*. 2009;44(4):239–248. doi:10.1007/s00535-009-0014-1
3. Pimentel-Nunes P, Libânio D, Marcos-Pinto R, et al. Management of epithelial precancerous conditions and lesions in the stomach (MAPS II): European society of gastrointestinal endoscopy (ESGE), European helicobacter and microbiota study group (EHMSG), European society of pathology (ESP), and sociedade portuguesa de endoscopia digestiva (SPED) guideline update 2019. *Endoscopy*. 2019;51(04):365–388. doi:10.1055/a-0859-1883

4. Jin DW, Li JR, Li Q. Research progress on chronic atrophic gastritis in traditional Chinese and Western medicine. *Chin J Ethnomed Ethnopharm*. 2021;30(21):72–75,83.
5. Zhang Y, Ding YY, Zhao Y, et al. Advances in traditional Chinese medicine treatment of chronic atrophic gastritis. *Acta Chin Med Pharmacol*. 2021;49(12):112–116. doi:10.19664/j.cnki.1002-2392.210299
6. Wang SK, Yin SP, Wang D, et al. Application of Zhishi Xiaopi Pill in digestive system diseases. *Hubei J Tradit Chin Med*. 2018;(10):58–62.
7. Dang MQ. Exploration of Professor Wang Daokun's medication rules in treating chronic atrophic gastritis precancerous lesions. Master's thesis. Gansu Univ Chin Med; 2016.
8. Cui C. Clinical observation of Zhishi Xiaopi Pill combined with lansoprazole enteric-coated tablets in treating chronic atrophic gastritis. *Tianjin Pharm*. 2024;(1):25–28.
9. Ren Y. Clinical value of modified Zhishi Xiaopi decoction combined with Danshen Drink in treating chronic atrophic gastritis. *Inner Mongolia J Tradit Chin Med*. 2024;(5):38–39. doi:10.16040/j.cnki.cn15-1101.2024.05.012
10. Zhang QQ, Liu NY, Wu D, et al. Molecular mechanisms of traditional Chinese medicine in treating gastric precancerous lesions based on data mining and network pharmacology. *J Zhejiang Univ*. 2022;51(5):573–584. doi:10.3724/zdxbyxb-2022-0278
11. Dong TX, Yu ZM. Effects of Astragalus polysaccharides on JAK1/STAT3 signaling pathway in rats with chronic atrophic gastritis. *Chin J Clin Pharmacol*. 2020;(22):3764–3768. doi:10.13699/j.cnki.1001-6821.2020.22.045
12. Cai TT, Lin L, Pan HF, et al. Protective effect of Panax notoginseng saponins on gastric mucosa in rats with gastric precancerous lesions via activation of JNK signaling pathway. *Chin J Tradit Chin Med Pharm*. 2019;34(12):5877–5880.
13. Xu CC, Su XL, Pan YY, et al. Mechanism of Hedyotis diffusa-Scutellaria barbata herb pair in treating gastric precancerous lesions based on network pharmacology. *Beijing J Tradit Chin Med*. 2021;(8):901–906. doi:10.16025/j.1674-1307.2021.08.028
14. Xie X, Wei Y. A review on anti-cancer properties of quercetin in gastric cancer. *Front Pharmacol*. 2025;16:1563229. doi:10.3389/fphar.2025.1563229
15. Hao X, Yuan S, Ning J, et al. Luteolin improves precancerous conditions of the gastric mucosa by binding STAT3 and inhibiting LCN2 expression. *Int J Biol Sci*. 2025;21(8):3397–3415. doi:10.7150/ijbs.111636
16. Li Q, Hu X, Xuan Y, et al. Kaempferol protects ethanol-induced gastric ulcers in mice via pro-inflammatory cytokines and NO. *ABBS*. 2018;50(3):246–253. doi:10.1093/abbs/gmy002
17. Ma J, Duan YQ, Gong ZH, et al. Professor Wang Daokun's experience in treating chronic atrophic gastritis with self-designed empirical formula. *Tradit Chin Med Res*. 2020;(9):38–40.
18. Mattoli L, Gianni M, Burico M. Mass spectrometry-based metabolomic analysis as a tool for quality control of natural complex products. *Mass Spectrom Rev*. 2023;42(4):1358–1396. doi:10.1002/mas.21773
19. Wang YN, Xu F, Zhang P, et al. MicroRNA-575 regulates development of gastric cancer by targeting PTEN. *Biomed Pharmacother*. 2019;113:108716. doi:10.1016/j.biopha.2019.108716
20. Rybstein MD, Bravo-San Pedro JM, Kroemer G, et al. The autophagic network and cancer. *Nat Cell Biol*. 2018;20(3):243–251. doi:10.1038/s41556-018-0042-2
21. Chen R, Zou J, Zhong X, Li J, Kang R, Tang D. HMGB1 in the interplay between autophagy and apoptosis in cancer. *Cancer Lett*. 2024;581:216494. doi:10.1016/j.canlet.2023.216494
22. Qian HR, Yang Y. Functional role of autophagy in gastric cancer. *Oncotarget*. 2016;7(14):17641–17651. doi:10.18632/oncotarget.7508
23. Zhou Y, Zhu J, Lu ZQ, et al. Expression and significance of PI3K/AKT pathway in gastric mucosa. *Mod Diagn Treat*. 2015;26(15):3371–3373.
24. Xie Y, Liu L. Analysis of correlation between HP infection and activation of PI3K/Akt pathway in mucosal tissues of gastric cancer and precancerous lesions. *Oncol Lett*. 2018;16(5):5615–5620. doi:10.3892/ol.2018.9329
25. Zhang ZM, Huang JQ, He BX, et al. Regulatory effects of shenbai granules on autophagy and apoptosis of gastric mucosal epithelial cells in patients with gastric precancerous lesions. *J Beijing Univ Tradit Chin Med*. 2022;45(10):1052–1059.
26. Lin L, Han T, Lu L, et al. Summary and review of animal models for chronic atrophic gastritis and gastric precancerous lesions. *Chin J Exp Tradit Med Form*. 2019;25(2):220–227. doi:10.13422/j.cnki.syfjx.20182329
27. Fang JY, Du YQ, Liu WZ, et al. Chinese consensus on chronic gastritis (2017, Shanghai). *Chin J Gastroenterol*. 2017;22(11):670–687.
28. Zhou WT, Shen H, Jiang YS, et al. Advances in experimental replication of gastric precancerous lesion animal models. *World Sci Technol-Mod Tradit Chin Med*. 2021;23(5):1439–1447.
29. Kim J, Kundu M, Viollet B, et al. AMPK and mTOR regulate autophagy through direct phosphorylation of Ulk1. *Nat Cell Biol*. 2011;13(2):132–141. doi:10.1038/ncb2152
30. Ganley IG, Lam DH, Wang J, et al. ULK1·ATG13·FIP200 complex mediates mTOR signaling and is essential for autophagy. *J Biol Chem*. 2009;284(18):12297–12305. doi:10.1074/jbc.M900573200
31. Dikic I, Elazar Z. Mechanism and medical implications of mammalian autophagy. *Nat Rev Mol Cell Biol*. 2018;19(6):349–364. doi:10.1038/s41580-018-0003-4
32. Fan ZW, Lu M, Fan XY. Correlation between dietary irregularities and chronic atrophic gastritis. *Shandong J Tradit Chin Med*. 2019;38(4):309–311,342. doi:10.16295/j.cnki.0257-358x.2019.04.003
33. Zhu XX, Shi LF, Wu XT, et al. Establishment of experimental chronic atrophic gastritis with spleen qi deficiency syndrome model and pathological changes at different stages. *Chin J Tradit Chin Med Pharm*. 2012;30(2):231–233,449–450. doi:10.13193/j.archtcm.2012.02.9zhuxx.004
34. Manthey JA, Guthrie N. Antiproliferative activities of citrus flavonoids against six human cancer cell lines. *J Agricultural Food Chemistry*. 2002;50(21):5837–5843. doi:10.1021/jf020121d
35. Chen ZH, Wei Y, An J, et al. Literature review on modeling methods for chronic atrophic gastritis and gastric precancerous lesions in rats. *Tianjin J Tradit Chin Med*. 2019;36(9):850–855.
36. Zheng JY, Zhao ZM, Pan HF, et al. Pathological and ultrastructural study of gastric mucosa in rats with spleen deficiency syndrome of gastric precancerous lesions. *Chin J Tradit Chin Med Pharm*. 2018;33(5):1730–1735.
37. Lu YT, Liu HY, Shang JJ, et al. Research progress on MNNG-induced composite modeling of gastric precancerous lesions in rats. *Chin J Chin Mater Med*. 2021;(16):4089–4095. doi:10.19540/j.cnki.cjcmm.20210316.601
38. Liang GY, Liu JF, Li H, et al. Effects of xinwei granules on gastric mucosa in rats with gastric precancerous lesions via STAT3/Survivin signaling pathway. *Liaoning J Tradit Chin Med*. 2022;(4):197–201,225. doi:10.13192/j.issn.1000-1719.2022.04.053

39. Liu Y, Yang QL, Han B, et al. Research progress on autophagy-regulated cell death by antitumor components of traditional Chinese medicine. *Acta Pharm Sin*. 2025;60(03):533–549. doi:10.16438/j.0513-4870.2024-0591
40. Hu XT, Ding C, Zhou N, et al. Quercetin protects gastric epithelial cell from oxidative damage in vitro and in vivo. *Eur J Pharmacol*. 2015;754:115–124. doi:10.1016/j.ejphar.2015.02.007
41. Shao YX, Luo WZ, Zhang H. Effect of quercetin regulating p53 expression on malignant behavior of gastric cancer cells. *Chin J Gerontol*. 2021;41(21):4803–4806.
42. Ji Y, Li L, Ma YX, et al. Quercetin inhibits growth of hepatocellular carcinoma by apoptosis induction in part via autophagy stimulation in mice. *J Nutr Biochem*. 2019;69:108–119. doi:10.1016/j.jnutbio.2019.03.018
43. Wang SY, Lin J, Xing LK, et al. Mechanism of resveratrol inhibiting proliferation of gastric cancer MGC803 cells via TGFβ1/Smad signaling pathway. *Mod Oncol*. 2016;(23):3713–3717.
44. Sun LH, Xia JG, Qian CH, et al. Resveratrol inhibits proliferation and migration of gastric cancer SGC-7901 cells via PI3K/AKT pathway. *Prog Mod Biomed*. 2016;(17):3237–3240,3267. doi:10.13241/j.cnki.pmb.2016.17.008
45. Wu X, Xu Y, Zhu B, et al. Resveratrol induces apoptosis in SGC-7901 gastric cancer cells. *Oncol Lett*. 2018;16(3):2949–2956. doi:10.3892/ol.2018.9045
46. Su W, Liu YP, Li ZK, et al. Genistein induces apoptosis in human gastric cancer BGC-823 cells and its molecular mechanism. *Chin Tradit Herb Drugs*. 2007;(6):874–878.
47. Tu W, Hong Y, Huang M, Chen M, Gan H. Effect of kaempferol on hedgehog signaling pathway in rats with --chronic atrophic gastritis – based on network pharmacological screening and experimental verification. *Biomed Pharmacother*. 2022;145:112451. doi:10.1016/j.biopha.2021.112451
48. Zhang N, Chen P, Liang X, et al. Luteolin targets the AGE-RAGE signaling to mitigate inflammation and ferroptosis in chronic atrophic gastritis. *Aging*. 2024;16(13):10918–10930. doi:10.18632/aging.205969
49. Imran M, Rauf A, Abu-Izneid T, et al. Luteolin, a flavonoid, as an anticancer agent: a review (vol 112, 108612, 2019). *Biomed Pharmacother*. 2019;(116):116.
50. Zhang CH, Huang B, Li J, et al. Mechanism of COX-2 and p53 in chronic atrophic gastritis and research progress in traditional Chinese medicine treatment. *Guangming J Chin Med*. 2017;32(16):2431–2434.
51. Xie YJ, Wang CX, Lin WQ, et al. Expression and correlation of Helicobacter pylori, COX-2 and p53 in gastric cancer and precancerous lesions. *Chin J Integr Tradit West Med Dig*. 2014;22(3):122–125.
52. Hu W, Chen S, Thorne RF, et al. TP53, TP53 Target Genes (DRAM, TIGAR), and Autophagy. *Adv Exp Med Biol*. 2019;1206:127–149.
53. Zhang XH, Sun JF. Research progress on traditional Chinese medicine monomers targeting PI3K/Akt signaling pathway for gastric cancer treatment. *Inner Mongolia J Tradit Chin Med*. 2024;(12):154–157. doi:10.16040/j.cnki.cn15-1101.2024.12.068
54. Gao P, Seebacher NA, Hornicek F, et al. Advances in sarcoma gene mutations and therapeutic targets. *Cancer Treat Rev*. 2018;62:98–109. doi:10.1016/j.ctrv.2017.11.001
55. Deng JY. STAT-3 correlates with lymph node metastasis and cell survival in gastric cancer. *WJG*. 2010;16(42):5380. doi:10.3748/wjg.v16.i42.5380
56. Judd LM, Menheniott TR, Ling H, et al. Inhibition of the JAK2/STAT3 pathway reduces gastric cancer growth in vitro and in vivo. *PLoS One*. 2014;9(5):e95993. doi:10.1371/journal.pone.0095993
57. Li Y, Li T, Chen J, et al. Manpixiao decoction halted the malignant transformation of precancerous lesions of gastric cancer: from network prediction to in-vivo verification. *Front Pharmacol*. 2022;13:927731. doi:10.3389/fphar.2022.927731
58. Giatromanolaki A, Koukourakis MI, Koutsopoulos AV, et al. Autophagy and hypoxia in colonic adenomas related to aggressive features. *Colorectal Dis*. 2013;15(5):e223–30. doi:10.1111/codi.12147
59. Zhang JX, Wang WB, Yan SG, et al. CagA and VacA inhibit autophagy of gastric mucosal epithelial cells and promote progression of gastric precancerous lesions. *J Cent South Univ Med Sci*. 2022;47(7):942–951.
60. Li TJ, Wei ST, Li H, et al. Effect of Anwei Decoction on apoptosis-related factors in chronic atrophic gastritis model rats. *Shaanxi J Tradit Chin Med*. 2018;39(8):987–990,994.
61. Zhao H, Zhou D, Chen Y, et al. Beneficial effects of Heqi san on rat model of polycystic ovary syndrome through the PI3K/AKT pathway. *DARU J Pharm Sci*. 2017;25(1):21. doi:10.1186/s40199-017-0188-7
62. Gong H, Lyu X, Liu Y, et al. Eupatilin inhibits pulmonary fibrosis by activating Sestrin2/PI3K/Akt/mTOR dependent autophagy pathway. *Life Sci*. 2023;334:122218. doi:10.1016/j.lfs.2023.122218
63. Morgos DT, Stefani C, Miricescu D, et al. Targeting PI3K/AKT/mTOR and MAPK signaling pathways in gastric cancer. *IJMS*. 2024;25(3):1848. doi:10.3390/ijms25031848
64. Cai T, Zhang C, Zeng X, et al. Protective effects of Weipixiao decoction against MNNG-induced gastric precancerous lesions in rats. *Biomed Pharmacother*. 2019;120:109427. doi:10.1016/j.biopha.2019.109427